β-decay branching ratios of the neutron-rich nucleus ^{15}B

R. Harkewicz and D. J. Morrissey
National Superconducting Cyclotron Laboratory and Department of Chemistry, Michigan State University, East Lansing, Michigan 48824

B. A. Brown and J. A. Nolen, Jr.
National Superconducting Cyclotron Laboratory and Department of Physics and Astronomy, Michigan State University, East Lansing, Michigan 48824

N. A. Orr, B. M. Sherrill, J. S. Winfield, and J. A. Winger
National Superconducting Cyclotron Laboratory, Michigan State University, East Lansing, Michigan 48824
(Received 13 August 1991)

We have used the Michigan State University National Superconducting Cylcotron Laboratory A1200 radioactive beam facility and a newly designed neutron detector array to measure the first β-delayed neutron spectrosopy of ^{15}B and the ^{15}B β-decay branch to ^{15}C bound states. The ^{15}B ions were produced as projectile fragments in the interaction of an $E/A=80$ MeV ^{18}O beam with a thick beryllium target. From these measurements, we deduce the ^{15}B β-decay branching ratios. The results are compared with shell-model predictions carried out in the *psd* model space.

I. INTRODUCTION

The neutron-rich boron nuclei have been studied over a long period of time. These nuclei are interesting in that the ratio of neutrons to protons lies in the range of two to almost three. ^{15}B was first observed to be stable against particle decay in 1966 [1].

In 1974 the particle stability of ^{17}B and the particle instability of ^{16}B were shown [2]. Recently, in 1984, ^{19}B was shown to be the most neutron-rich stable boron isotope; in that same experiment ^{18}B was shown to be unstable to prompt neutron emission [3]. Thus progress in establishing the limits of particle stability for the boron isotopes has been quite good, but surprisingly little detailed information is known about the decay of ^{15}B. The half-life is known to be 10.5 ± 0.3 ms [4] and the decay is dominated by delayed single neutron emission ($P_{0n}<5\%$ and $P_{2n}<1.5\%$) [5]. However, no measurement of the β-delayed neutron energies has been made; hence the β-decay branching ratios of ^{15}B to states in ^{15}C are not known. Detailed experimental information on the β-decay properties of nuclei far from stability are particularly important because they can provide crucial tests of the validity of shell-model Hamiltonians which have been constructed from data associated with stable and near-stable nuclei and can lead to refinement of shell-model interactions. With such refinements, the shell-model extrapolations for the properties of even more exotic nuclei become, of course, more reliable. These extrapolations are important in understanding the unusual properties of the most neutron-rich nuclei—such as the shell inversion in the ^{31}Mg mass region [6] and the large neutron radii for the Li and Be isotopes [7], as well as understanding the role of very neutron-rich nuclei in the astrophysical rapid-neutron capture process.

We also note that ^{15}B, with $P_n\approx100\%$, has been used as an efficiency standard for neutron detectors in other β-delayed neutron measurements; such calibrations depend somewhat on the assumed neutron energy distribution [8,9]. A measurement of the neutron energy spectrum for ^{15}B is important for establishing the utility of ^{15}B as such a standard.

We present here the first β-delayed neutron spectroscopy of ^{15}B and introduce the recently constructed neutron detector array, a device designed for the study of β-delayed neutron emitting nuclei. We report the β-decay branching ratios of ^{15}B as well as a remeasurement of its half-life. Our results are compared to shell-model calculations carried out in the *psd* model space with the Millener-Kurath-Wildenthal interaction [10].

Section II describes production and separation of ^{15}B using the Michigan State University National Superconducting Cyclotron Laboratory (MSU NSCL) A1200 radioactive beam device, the experimental setup and the neutron detector array. The experimental results and analysis are discussed in Sec. III. In Sec. IV we present shell-model predictions of the ^{15}B β-decay and compare them with the experimental results.

II. EXPERIMENTAL DETAILS

The ^{15}B nuclei observed in this work were produced at the National Superconducting Cyclotron Laboratory at Michigan State University with an $E/A=80$ MeV ^{18}O beam, with an intensity of 12 particle nA, from the K1200 Cyclotron. A ^{9}Be target, 790 mg/cm^2 thick, was used and the reaction products were separated using the momentum-loss achromat mode of the NSCL A1200. A full description of the A1200 separator is provided in Ref. [11]. In the present experiment, the selection of

heavy-ion reaction products was made by combining magnetic selection of all products with $m/q = 3$ and the energy loss in an achromatic wedge (aluminum, median thickness 365 mg/cm^2, angle 2.8 mrad). The wedge introduces a Z-dependent momentum shift that is converted into a physical separation of the isotopes at the focal plane by the dipole magnets. In this experiment, the A1200 provided a nearly pure (>94%) beam of $^{15}B^{5+}$ ions at the final image; the impurities were $^{9}Li^{3+}$ and $^{6}He^{2+}$ and $^{3}H^{+}$. The ^{15}B beam was then transported through a beam line to a low background experimental vault, some 60 m away (including a total of 3 m of concrete shielding) from the site of the primary ^{18}O reaction, with an overall yield of approximately 600 particles per second.

The boron ions were stopped in an active detector in the center of an array of neutron detectors. A schematic view of the NSCL neutron detector array is shown in Fig. 1. The ^{15}B beam ($E/A \approx 60$ MeV) passed through a thin Kapton window (0.25-mm thick) that separated the vacuum of the beam line from the air, approximately 1 m of air, 6.8 mm of aluminum degrader (exiting with $E/A \approx 25$ MeV), a silicon surface-barrier ΔE detector (0.2-mm thick, 300-mm^2 area), and came to rest in the center (0.5 cm) of a thin plastic scintillator, referred to as the *implantation detector* (BC412, 2-cm square by 1-cm deep). Energy loss in the ΔE detector, in addition to a time-of-flight measurement, allowed on-line monitoring of the purity of the ^{15}B secondary beam; the ΔE detector also allowed us to determine the exact number of ^{15}B ions deposited in the implantation detector. A thick silicon surface-barrier veto detector (1-mm thick, 300-mm^2 area) was placed behind the implantation detector in order to verify that the ^{15}B ions were indeed stopped in the plastic material.

As indicated in Fig. 1, the implantation detector was partially surrounded by 16 large area (157 cm by 7.6 cm by 2.54 cm thick, each) BC412 plastic neutron detectors bent in a 1-m radius of curvature. The gap between adjacent neutron detectors had an area of approximately 800 cm^2. Neutrons leaving the central implantation detector and interacting with any part of any one of the 16 neutron detectors would have a uniform flight path of 1 m. The 16 detectors covered a total solid angle of approximately 1.9 sr.

The production rate of ^{15}B was sufficiently high that the cyclotron beam was cycled on and off, discussed below, and neutrons were observed during the beam-off period. The β decay of the ^{15}B was detected by two photomultiplier tubes (1.9-cm diameter HAMAMATSU H3167) attached to the implantation detector. The calculated mean-time of these signals served as the start for the neutron time-of-flight measurement. Each neutron detector also had two photomultiplier tubes (7.6-cm diameter, THORN EMI 9821B) and the mean-time served as a neutron time-of-flight stop.

A. Cyclotron beam on/beam off cycle

In order to study the decay of ^{15}B it was necessary to pulse the primary beam on and off for fixed intervals of time. This was accomplished with a gate module that periodically sent a logic signal to a fast phase shifter in the rf transmitter of one of the "dees" of the K1200 cyclotron. The cyclotron beam was interrupted within approximately 40 μsec [12]. To measure the decay branches of ^{15}B to neutron-unbound states in ^{15}C a 50 ms on/50 ms off cycle was used for part of the experiment and later was changed to a 20 ms on/40 ms off cycle. ^{15}B ions were deposited in the implantation detector during

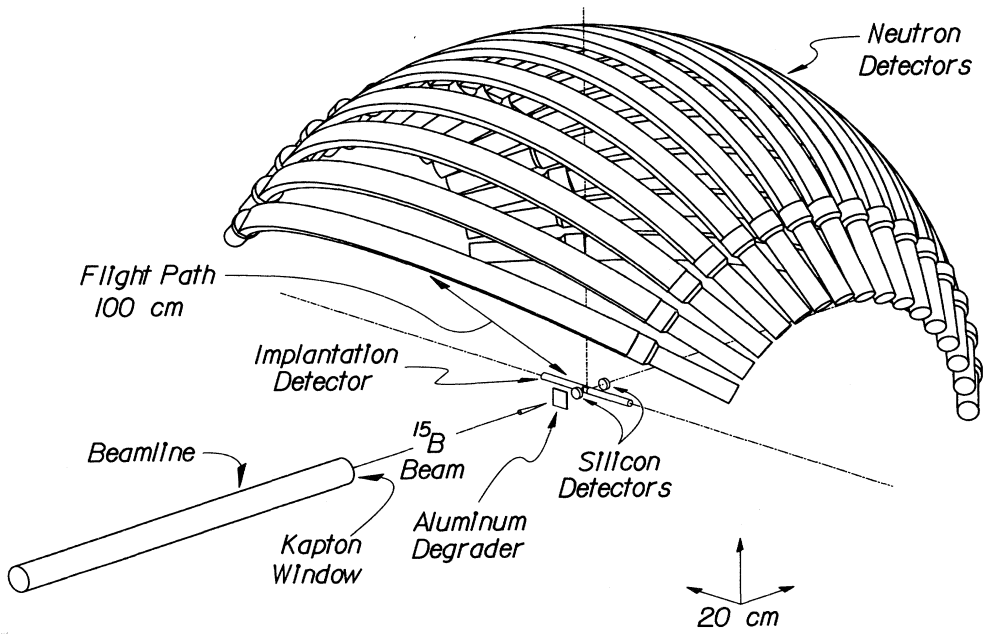

FIG. 1. Schematic drawing of the neutron detector array and the experimental setup.

the beam-on time and decays were monitored during the subsequent beam-off time. A real time clock module started at the beginning of each beam-off interval (zeroed at the beginning of each subsequent beam-on interval) was used to measure the time of each event relative to the end of the beam-on period. The total beam-off period was easily measured with the real time clock. The beam-on period was calibrated by recording events from a γ-ray source positioned near the implantation detector (during these runs there was no cyclotron beam) for the two different time cycles. By ratio the exact times of the cycles turned out to be 49.23 ms on/49.80 ms off and 20.33 ms on/39.55 ms off.

In order to determine the number of ^{15}B decays that led to bound states in ^{15}C ($t_{1/2}=2.449$ s, Ref. [4]) the cyclotron beam cycle was later changed to 4.847 s on/5.719 s off. Here, ^{15}B ions were deposited in the implantation detector during the beam on period and ^{15}C decays (β emission) were counted during the beam-off period.

B. Neutron detector efficiency

The neutron detection efficiency of the neutron array was determined as a function of threshold setting using a plutonium-beryllium neutron source (PuBe source) positioned at the center of the detector array. In addition, a small liquid scintillation detector (BC501, 6.75 cm diameter by 3.60 cm deep), whose efficiency could be reliably determined to within 10% using a Monte Carlo efficiency code [13], was also placed a distance of 1 m from the PuBe source to be used as a standard in our efficiency calibration. This source produces neutrons in coincidence with a 4.4-MeV γ ray through the ^{9}Be(^{4}He,n)^{12}C* reaction. The 4.4-MeV γ ray was detected in a 5-cm diameter by 10-cm deep BaF_2 detector and served as a time-of-flight start signal. Neutron time-of-flight spectra were obtained for each of the 16 detectors in addition to the small "standard" detector. By taking the ratio of number of neutrons detected in the large and small detectors as a function of energy we were able to determine the efficiency of each of our array detectors for neutrons with kinetic energies in the range of 1.7 to 5.0 MeV. A collimated ^{60}Co γ-ray source, which yields a Compton edge of approximately 1 MeV, was placed at different locations along each neutron detector (varying distances from the photomultiplier tubes) in order to determine the detector threshold and its dependence on position. A Monte Carlo efficiency calculation [13] was performed for an array detector using an *average* threshold of 125 keV electron-equivalent energy. The results of the efficiency calibration and Monte Carlo calculation are shown in Table I for the detection of neutrons in one of the curved neutron detectors (not including solid angle). The overall agreement is quite good.

TABLE I. Comparison of measured and calculated efficiencies for neutron array detector as a function of neutron energy.

Energy (MeV)	Measured (PuBe)	Calculated (Monte Carlo)
1.8	22.5%	22.0%
3.0	21.8%	20.8%
4.5	18.0%	18.8%

III. RESULTS

The decay for ^{15}B inclusive β emission from the 20 ms/40 ms beam cycle is shown in Fig. 2. The half-life of 10.4±0.2 ms was obtained from a least-squares fitting procedure assuming a single exponential decay component and a constant background. This value is in excellent agreement with previous measurements [4]. In addition, a half-life of 10.5±0.4 ms was obtained from a similar measurement requiring β-neutron coincidence.

The decay curve observed from the 5 s/6 s beam cycle is shown in Fig. 3. The first 375 ms after the beam was stopped are not included to allow the ^{15}B nuclei to decay. This measurement was more sensitive to the longer-lived impurities ^{6}He ($t_{1/2}=0.807$ s) [14] and ^{9}Li ($t_{1/2}=0.178$ s) [14]. Inclusion of these impurities plus a very long-lived background as components in our fitting procedure yielded an initial ^{15}C ($t_{1/2}=2.449$ s) [4] count rate of 7060/s resulting from the implantation of 14.551×10^{6} ^{15}B ions. To determine the β-decay branch of ^{15}B to bound states in ^{15}C (ground state and 0.740-MeV state), it is necessary to know the efficiency of the implantation detector for ^{15}C β decay. To determine this we first considered the implantation detector efficiency for ^{15}B β decay. Incorporating the exact times of the beam on/beam off cycles and the exact number of ^{15}B ions implanted in the detector, we determined this efficiency to be

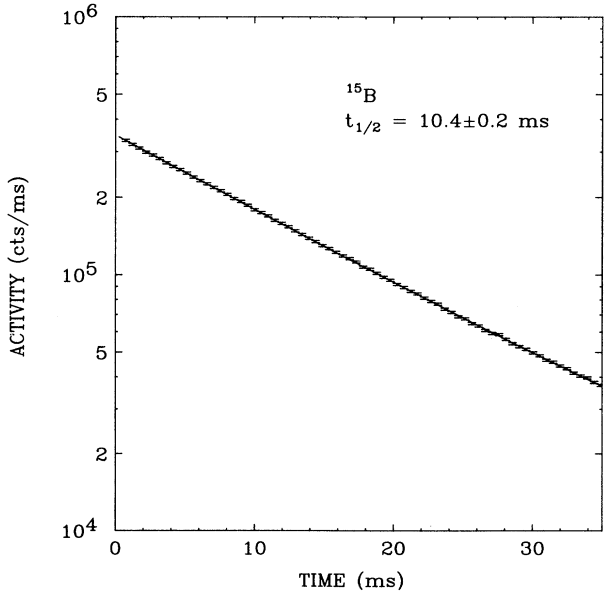

FIG. 2. Experimental decay curve for ^{15}B from the 20 ms on/40 ms off beam cycle. Solid line corresponds to a single-component fit plus a constant background.

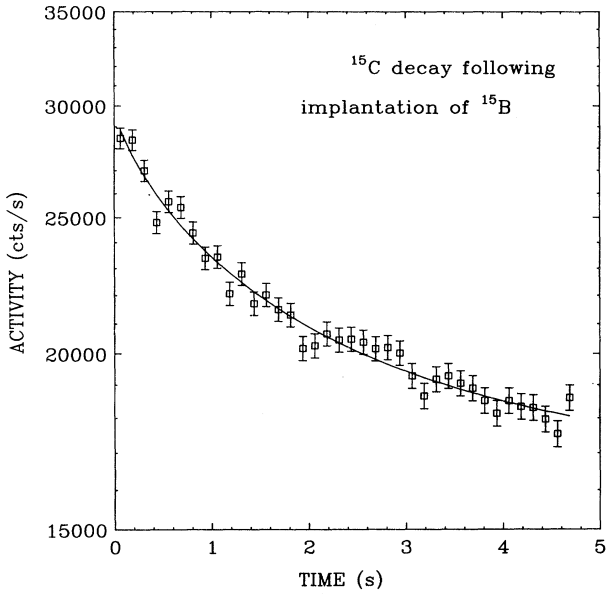

FIG. 3. Experimental decay curve from the 5 s on/6 s off beam cycle following the implantation of ^{15}B. Solid line corresponds to a three-component fit (^{6}He, ^{9}Li, ^{15}C) plus a long-lived background. This decay curve is used to determine the ^{15}B β-decay branch to ^{15}C bound states.

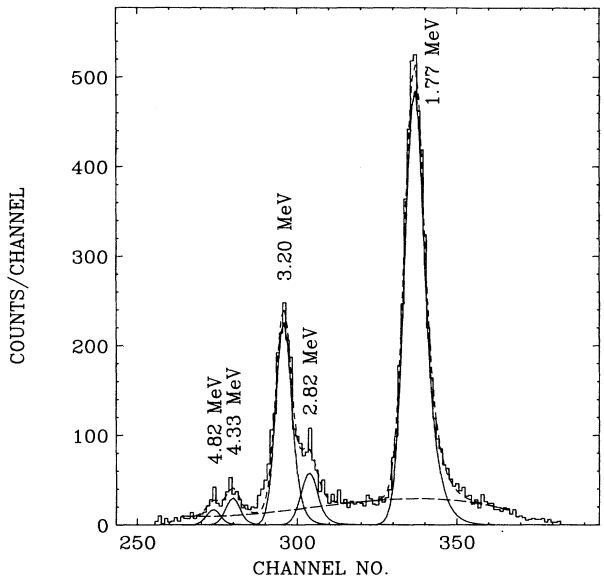

FIG. 4. Delayed neutron time-of-flight spectrum for one of the 16-array detectors. The five unfolded β-delayed neutron peaks are shown. The spectrum is not corrected for neutron efficiency. The fits to individual peaks are indicated with solid lines, the background by long dashes, and the sum of all contributions by short dashes.

80.5±2.5%. This efficiency was determined separately for the two different beam on/beam off cycles and both were in close agreement (within 2%). Thus, by considering that (1) the β decay of the ^{15}B parent and ^{15}C daughter atoms took place at the same location inside the implantation detector, (2) the average β-particle energy is approximately 0.35 $E_{\max}$ and β particles of this average energy from ^{15}B and ^{15}C differ by only 5% in their dE/dx in plastic [15], and (3) the low-energy threshold setting of the implantation detector (100 keV), we conclude the implantation detector had the same efficiency for ^{15}B and ^{15}C β decays.

Incorporating the exact time of our beam on/beam off cycle, the exact number of ^{15}B ions implanted in the detector, the measured initial count rate of the ^{15}C β decays and the detector β efficiency we determined the ^{15}B β-decay branch to ^{15}C bound states to be 0.32±0.08%. This measurement is in agreement with, though significantly lower than the limit of $P_{0n} < 5\%$ established by Dufour *et al.* [5].

The neutron time-of-flight spectrum for one of our 16 array detectors is presented in Fig. 4. A peak resulting from relativistic electrons that traveled from the implantation detector to the neutron detector (i.e., the β decay of ^{15}B), appeared in the spectrum, not shown in Fig. 4, and was centered at channel 186.6 and established time-zero. The neutron energies were deduced from the known flight path of 100 cm and accurate time calibration (using an electronic time calibrator) of 0.3428ns/channel. The program PHAEDRUS [16] was used to fit simultaneously the five β-delayed neutron peaks.

The low level, negative parity states of ^{15}C have level widths on the order of 10 to 40 keV [4] (small compared to the peak width caused by instrumentation), and therefore the width of each peak was determined from the total time uncertainty, a combination of 1.0 ns from the electronics and a neutron-energy-dependent time uncertainty owing to a flight path uncertainty of 4.1 cm. A smooth polynomial function was fit through the regions of the spectrum with no peaks for the background. The background consisted of (1) a constant level throughout the entire spectrum resulting from random coincidence events and (2) a steadily increasing level toward the low-energy end of the spectrum resulting from decay neutrons that did not travel directly from the implantation detector to the neutron detector. A similar fitted spectrum was obtained for each of the other fifteen neutron detectors.

From these spectra transitions to five neutron-unbound states in ^{15}C were observed. A β-decay branch leading to one neutron emission via the first excited state of ^{14}C at 6.08 MeV (compared to the five observable peaks resulting from decays via the ^{14}C ground state) requires the excitation energy of ^{15}C to be at least 7.31 MeV and would result in distinct neutron energy peaks; no evidence for such peaks could be found in any of the 16 spectra. The β decay of ^{15}B to states in ^{15}C resulting in two neutron emission ($^{15}C^{*} \rightarrow {}^{13}C_{g.s.} + 2n$) requires the excitation energy of ^{15}C to be at least 9.39 MeV. Dufour *et al.* [5] have established an upper limit for two-neutron emission of less than 1.5%. We would expect less than one two-neutron event per detector pair for a 1.5% branch given

the total number of ^{15}B nuclei implanted in the array (5.083×10^6). Random coincidence events were observed at a level of 3–4 per detector pair. Therefore, accounting for the measured 0.32% decay branch to ^{15}C bound states, we conclude that $99.68^{+0.08}_{-1.58}$% of the ^{15}B β decays populate the five lowest negative parity states in ^{15}C (the five observable neutron peaks). This is the basis on which we determine the ^{15}B β-decay branching ratios and include the upper limit of 1.5% for two neutron emission into the errors of these calculated branching ratios.

After normalization for neutron efficiencies, correction for the neutron recoil energy and neutron binding energy of 1.218 MeV [4] the ^{15}B β-decay branching ratios were obtained by taking the mean value of the 16 separate detector results and are listed in Table II. The decay scheme of ^{15}B established on the basis of these results is shown in Fig. 5.

The low level states of ^{15}C are well documented (see Table 2, [4]). It is clear, considering the calculated logft values, that the five neutron peaks observed in this experiment all represent allowed decays to negative parity states in ^{15}C ($J^\pi=\frac{3}{2}^-$ for ^{15}B [4]; decays to the ground state and first excited state of ^{15}C (both positive parity states) represent first-forbidden decays. In addition, the 62.9%, 7.9%, 22.9%, and 4.1% observed branches correspond to the [E_x (MeV), J^π] 3.103, $\frac{1}{2}^-$; 4.220, $\frac{5}{2}^-$; 4.657, $\frac{3}{2}^-$; and 5.866, $\frac{1}{2}^-$ known ^{15}C states, respectively. The state observed at 6.38±0.06 MeV could represent the 6.358±0.006 or the 6.417±0.006 MeV known states in ^{15}C or, of course, a mixture of both. It should be noted that the literature lists only possible J^π assignments for these latter states; since our measurement suggests these are allowed transitions, this would restrict the state's J^π to be $\frac{1}{2}^-$, $\frac{3}{2}^-$, or $\frac{5}{2}^-$.

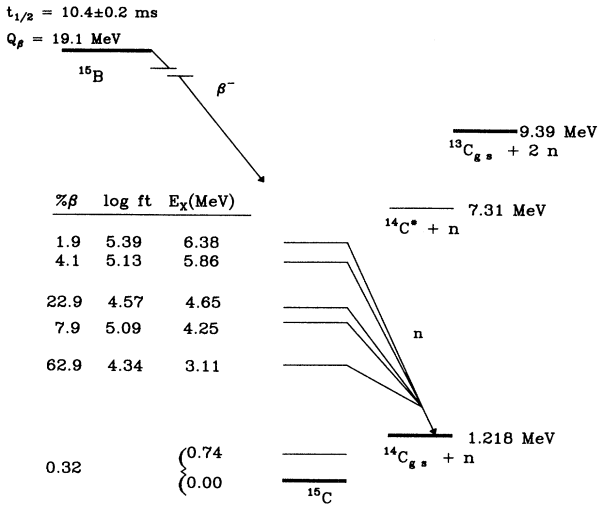

FIG. 5. Decay scheme of ^{15}B deduced from this work.

IV. DISCUSSION

For ^{15}B the dominant decay mode is through Gamow-Teller β decay. Table III is a comparison of our experimentally determined ^{15}B Gamow-Teller β-decay strengths to those predicted by our shell-model calculations for mass 15. Also included are the experimentally determined ^{15}C levels populated by ^{15}B β decay deduced from this work and those predicted by the shell model. The β-decay B(GT) values given in Table III are calculat-

TABLE II. Neutron energies, measured ^{15}C states (this work), known ^{15}C states [4], β branching, and logft values in ^{15}B decay. All energies are in MeV.

E_n	^{15}C (E_x) (this work)	^{15}C(E_x,J^π) (Ajzenberg-Selove[a])	I_β (%)	logft
4.82±0.06	6.38±0.06	6.358±0.006 $\frac{5}{2}^-,\frac{7}{2}^+,\frac{9}{2}^+$ 6.417±0.006 $\frac{3}{2}^-,\frac{5}{2}^-,\frac{7}{2}^-$	1.9±0.5	5.39±0.13
4.33±0.04	5.86±0.04	5.866±0.008 $\frac{1}{2}^-$	4.1±0.9	5.13±0.10
3.20±0.01	4.65±0.01	4.657±0.009 $\frac{3}{2}^-$	22.9±1.2	4.57±0.02
2.82±0.02	4.24±0.02	4.220±0.003 $\frac{5}{2}^-$	7.9±1.6	5.09±0.09
1.77±0.01	3.11±0.01	3.103±0.004 $\frac{1}{2}^-$	62.9±2.4	4.34±0.02
(neutron bound states in ^{15}C)	—	0.740 $\frac{5}{2}^+$ g.s. $\frac{1}{2}^+$	0.32±0.08	—

[a]Reference [4].

TABLE III. Measured and predicted Gamow-Teller β-decay strengths to the lowest $\frac{1}{2}^-$, $\frac{5}{2}^-$, $\frac{3}{2}^-$, $\frac{1}{2}^-$, and $\frac{5}{2}^-$[a] states in mass 15; also included are the measured and predicted energy levels of ^{15}C populated. (BR) denotes branching ratio. All energies are in MeV.

State		^{15}B (this work)		$A=15$ shell-model calculations	
J^π	BR (%)	^{15}C (E_x)	B(GT)[b]	^{15}C(E_x)	B(GT)
$\frac{1}{2}^-$	62.9±2.4	3.11±0.01	0.282±0.012	3.105	0.312
$\frac{5}{2}^-$	7.9±1.6	4.24±0.02	0.050±0.010	4.876	0.022
$\frac{3}{2}^-$	22.9±1.2	4.65±0.01	0.166±0.007	5.757	0.112
$\frac{1}{2}^-$	4.1±0.9	5.86±0.04	0.046±0.010	6.333	0.010
$\frac{5}{2}^-$[a]	1.9±0.5	6.38±0.06	0.025±0.006	6.881	0.001

[a]Shell-model calculations predict a $J^\pi=\frac{5}{2}^-$ state following the $\frac{1}{2}^-$ state. Experimentally, there is uncertainty as to the J^π of this state (see last paragraph of Sec. III).
[b]B(GT) values calculated from Eq. (1) of Sec. IV.

ed using the following expression:

$$B(\mathrm{GT})=\frac{6177\ \mathrm{s}}{ft}\ . \tag{1}$$

The theoretical Gamow-Teller β-decay strengths predicted here for mass 15 were carried out in the *psd* model space, within the framework of a spherical shell-model formalism [6], with the Millener-Kurath-Wildenthal interaction [10] in which the $0p_{3/2}$, $0p_{1/2}$, $0d_{5/2}$, $1s_{1/2}$, and $0d_{3/2}$ orbitals are active. Details concerning the manner in which the residual-interaction matrix elements and cross-shell matrix elements were determined are given in Ref. [10]. Single-particle energies were chosen to reproduce single-hole states in $A=15$ nuclei with the assumption of a closed $0s$-$0p$ shell configuration for ^{16}O. These theoretical B(GT) values include the $(g_a/g_v)^2$ factor and have been multiplied by a factor of 0.6 to take into account the empirical quenching observed for Gamow-Teller decay strengths in *sd*-shell nuclei [17].

Referring to Table III, agreement between the experimentally determined and theoretically predicted Gamow-Teller β-decay strengths is quite good for the largest decay branch (62.9% branch to the 3.11-MeV, $\frac{1}{2}^-$ state) while the shell-model underestimates the strengths to the higher level states. This might indicate the need to expand the model space in order to accommodate the higher level states. In this model space the active protons occupy the $0p$ shell and the active neutrons occupy the $1s0d$ shell. Half-life [10] as well as other Gamow-Teller β-decay strength [18] discrepancies between the model and experimental data have been associated with this type of configuration, and a better determination of the cross-shell residual interaction connecting the $0p$ and $1s0d$ orbitals might improve this situation.

In addition, the model calculations predict a total decay branch of less than 0.8% to all the remaining negative parity states in ^{15}C (states lying above the first five negative parity states), and this is in agreement with the experimental results. The first-forbidden beta-decay branching ratio was calculated with the *psd* wave functions using the Behrens-Buhring formulation [19] as explicated by Warburton *et al.* [20]. The results obtained with harmonic-oscillator radial wave functions are a branch of 0.53% to the $\frac{1}{2}^+$ ground state and 0.52% to the $\frac{5}{2}^+$ first excited state. The results obtained with Woods-Saxon wave functions are 0.23% to the ground state and 0.23% to the first excited state. The latter value for the total calculated branching ratio of 0.46% is in reasonable agreement with the experimental value of 0.32±0.08%. The large difference between the harmonic-oscillator and Woods-Saxon results is typical of sensitivity found for transitions between the s and p single-particle states in light nuclei [21].

V. CONCLUSION

We have reported on the first β-delayed neutron spectroscopy of ^{15}B using a newly constructed neutron detector array. We have established the population of five β-delayed neutron emitting states in ^{15}C in addition to measuring the the decay branch to ^{15}C bound states and have deduced the β-decay branching ratios and Gamow-Teller β-decay strengths of ^{15}B. The agreement with the shell-model predictions for the β decay of ^{15}B using the Millener-Kurath-Wildenthal interaction is, overall, quite good. We feel that a better determination of the cross-shell residual interactions might improve its β-decay description of exotic nuclei.

With the demonstration of the recently built neutron detector array for studying β-delayed neutron emitting nuclei, we are confident its future use in other β-decay studies of nuclei far from stability will provide valuable information against which the shell-model calculations can be vigorously tested.

ACKNOWLEDGMENTS

We would like to thank the entire staff of the NSCL, especially R. Blue, A. Galonsky, D. Sackett, D. Swan, and R. Swanson, for their valuable assistance regarding this work. This work is supported in part by the National Science Foundation under Grant No. PHY89-13815.

[1] A. M. Poskanzer, S. W. Cosper, E. K. Hyde, and J. Cerny, Phys. Rev. Lett. **17**, 1271 (1966).
[2] J. D. Bowman, A. M. Poskanzer, R. G. Korteling, and G. W. Butler, Phys. Rev. C **9**, 836 (1974).
[3] J. A. Musser and J. D. Stevenson, Phys. Rev. Lett. **53**, 2544 (1984).
[4] F. Ajzenberg-Selove, Nucl. Phys. **A523**, 1 (1991).
[5] J. P. Dufour, S. Beraud-Sudreau, R. Del Moral, H. Emmermann, A. Fleury, F. Hubert, C. Poinot, M. Pravikoff, J. Frehaut, M. Beau, A. Bertin, G. Giraudet, A. Huck, G. Klotz, C. Miehe, C. Richard-Serre, and H. Delagrande, Z. Phys. A **319**, 237 (1984).
[6] B. H. Wildenthal, M. S. Curtin, and B. A. Brown, Phys. Rev. C **28**, 1343 (1983).
[7] I. Tanihata, H. Hamagaki, O. Hashimoto, Y. Shida, N. Yoshikawa, K. Sugimoto, O. Yamakawa, T. Kobayashi, and N. Takahashi, Phys. Rev. Lett. **55**, 2676 (1985).
[8] M. Lewitowicz, Y. E. Penionzhkevich, A. G. Artukh, A. M. Kalinin, V. V. Kamanin, S. M. Lukyanov, N. H. Chau, A. C. Mueller, D. Guillemaud-Mueller, R. Anne, D. Bazin, C. Detraz, D. Guerreau, M. G. Saint-Laurent, V. Borrel, J. C. Jacmart, F. Pougheon, A. Richard, and W. D. Schmidt-Ott, Nucl. Phys. **A496**, 477 (1989).
[9] A. C. Mueller, D. Bazin, W. D. Schmidt-Ott, R. Anne, D. Guerreau, D. Guillemaud-Mueller, M. G. Saint-Laurent, V. Borrel, J. C. Jacmart, F. Pougheon, and A. Richard, Z. Phys. A **330**, 63 (1988).
[10] M. S. Curtin, L. H. Harwood, J. A. Nolen, Jr., B. Sherrill, Z. Q. Xie, and B. A. Brown, Phys. Rev. Lett. **56**, 34 (1986).
[11] B. M. Sherrill, D. J. Morrissey, J. A. Nolen, Jr., and J. A. Wigner, Nucl. Instrum. Methods Phys. Res. **B56/57**, 1106 (1991).
[12] D. Mikolas, B. A. Brown, W. Benenson, L. H. Harwood, E. Kashy, J. A. Nolen, Jr., B. M. Sherrill, J. Stevenson, J. S. Winfield, Z. Q. Xie, and R. Sherr, Phys. Rev. C **37**, 766 (1988).
[13] R. A. Cecil, B. D. Anderson, and R. Madey, Nucl. Instrum. Methods **161**, 439 (1979).
[14] F. Ajzenberg-Selove, Nucl. Phys. **A490**, 1 (1988).
[15] L. Pages, E. Bertel, H. Joffre, and L. Sklavenitis, At. Data **4**, 1 (1972).
[16] H. W. Schuh, PHAEDRUS, Institut fur Kerphysik der Universitat zu Koeln (1983) (unpublished).
[17] B. A. Brown and B. H. Wildenthal, Annu. Rev. Part. Sci. **38**, 29 (1988).
[18] K. A. Snover, E. G. Adelberger, P. G. Ikossi, and B. A. Brown, Phys. Rev. C **27**, 1837 (1983).
[19] H. Behrens and W. Buhring, Nucl. Phys. **A162**, 111 (1972); *Electron Radial Wave Functions and Nuclear β-Decay* (Clarenson Press, Oxford, 1982).
[20] E. K. Warburton, J. A. Becker, B. A. Brown, and D. J. Millener, Ann. Phys. (N.Y.) **187**, 471 (1988).
[21] D. J. Millener, D. E. Alburger, E. K. Warburton, and D. H. Wilkinson, Phys. Rev. C **26**, 1167 (1982).